

Structural and electrical properties of  $\text{Co}_{1-x}\text{Ru}_x\text{Sb}_2$ T. Harada<sup>a,\*</sup>, T. Kanomata<sup>a</sup>, T. Suzuki<sup>a</sup>, H. Yoshida<sup>b</sup>, T. Kaneko<sup>b</sup><sup>a</sup>Faculty of Engineering, Tohoku Gakuin University, Tagajo 985-8537, Japan<sup>b</sup>Institute for Materials Research, Tohoku University, Sendai 980-8577, Japan**Abstract**

Electrical resistivity, Hall coefficient, thermoelectric power and crystal structure were measured for the pseudo-binary system  $\text{Co}_{1-x}\text{Ru}_x\text{Sb}_2$ . By the results of X-ray analysis, the monoclinic distortion from the orthorhombic marcasite structure decreases gradually and disappears at about  $x=0.14$ . The electrical measurements show that  $\text{Co}_{1-x}\text{Ru}_x\text{Sb}_2$  ( $0 \leq x \leq 1$ ) are all semiconductive, in spite of the gradual change of valence electron number, by substituting Ru atom for Co. It was found that  $\log \rho$  of the samples for  $0.1 \leq x \leq 0.9$  exhibit  $T^{-1/4}$  and  $T^{-1/2}$  temperature dependence in the lower temperature range. These temperature changes of  $\rho$  are the same as those of the variable range hopping (VRH) conduction in the impurity conduction range of the usual semiconductors. © 2001 Elsevier Science B.V. All rights reserved.

**Keywords:**  $\text{Co}_{1-x}\text{Ru}_x\text{Sb}_2$ ; Electrical resistivity; Hall coefficient; Thermoelectric power; Crystal structure; Hopping conduction

**1. Introduction**

Transition metal dipnictide  $\text{RuSb}_2$  crystallizes in the orthorhombic marcasite structure (Fig. 1) [1,2] and  $\text{CoSb}_2$  in the monoclinic arsenopyrite type, slightly distorted from the marcasite structure [3,4]. These compounds are semiconductive and non-magnetic [5–8]. There have been many studies on some physical properties and the electronic structure of  $\text{CoSb}_2$  [9–12]. The semiconductive property of  $\text{CoSb}_2$  has been understood by the band model, that is, the cation  $e_g$  orbitals and the anion  $s$  and  $p$  orbitals form bonding  $\sigma$  and antibonding  $\sigma^*$  bands; the cation  $t_{2g}$  orbitals form narrow non-bonding bands located in the gap between  $\sigma$  and  $\sigma^*$  [11]. The five 3d electrons fill the non-bonding bands split by the monoclinic distortion. For  $\text{RuSb}_2$  it can be considered that the four 4d electrons fill the non-bonding d-bands split by the orthorhombic symmetry similar to  $\text{FeSb}_2$  in Ref. [12].

The purpose of the present investigation is to examine the complete mutual solubility between  $\text{CoSb}_2$  and  $\text{RuSb}_2$  and the transition from the monoclinic structure to the orthorhombic one, in order to ascertain the electrical properties of the pseudo binary system  $\text{Co}_{1-x}\text{Ru}_x\text{Sb}_2$ .

**2. Experimental**

Appropriate amounts of Co (4N pure), Ru (3N pure) and Sb (5N pure) powders (High Purity Chemicals, Japan)

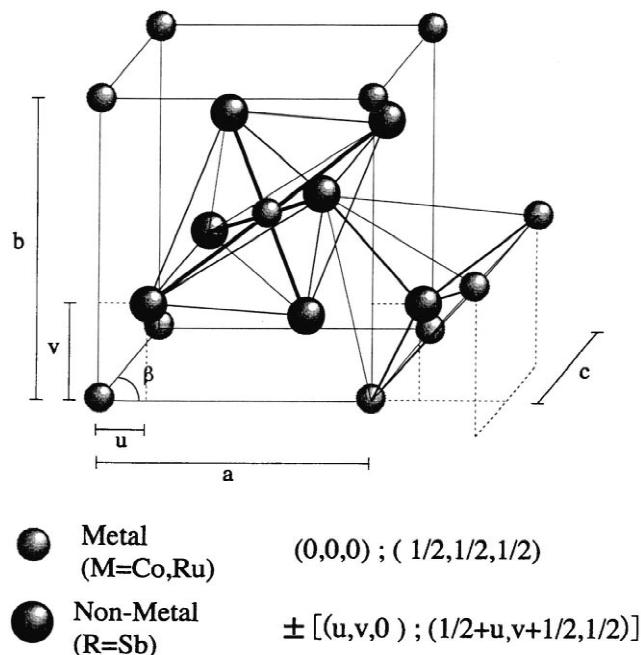


Fig. 1. Crystal structure of the orthorhombic marcasite-type.

\*Corresponding author. Fax: +81-22-368-7070.

E-mail address: tharada@tjcc.tohoku-gakuin.ac.jp (T. Harada).

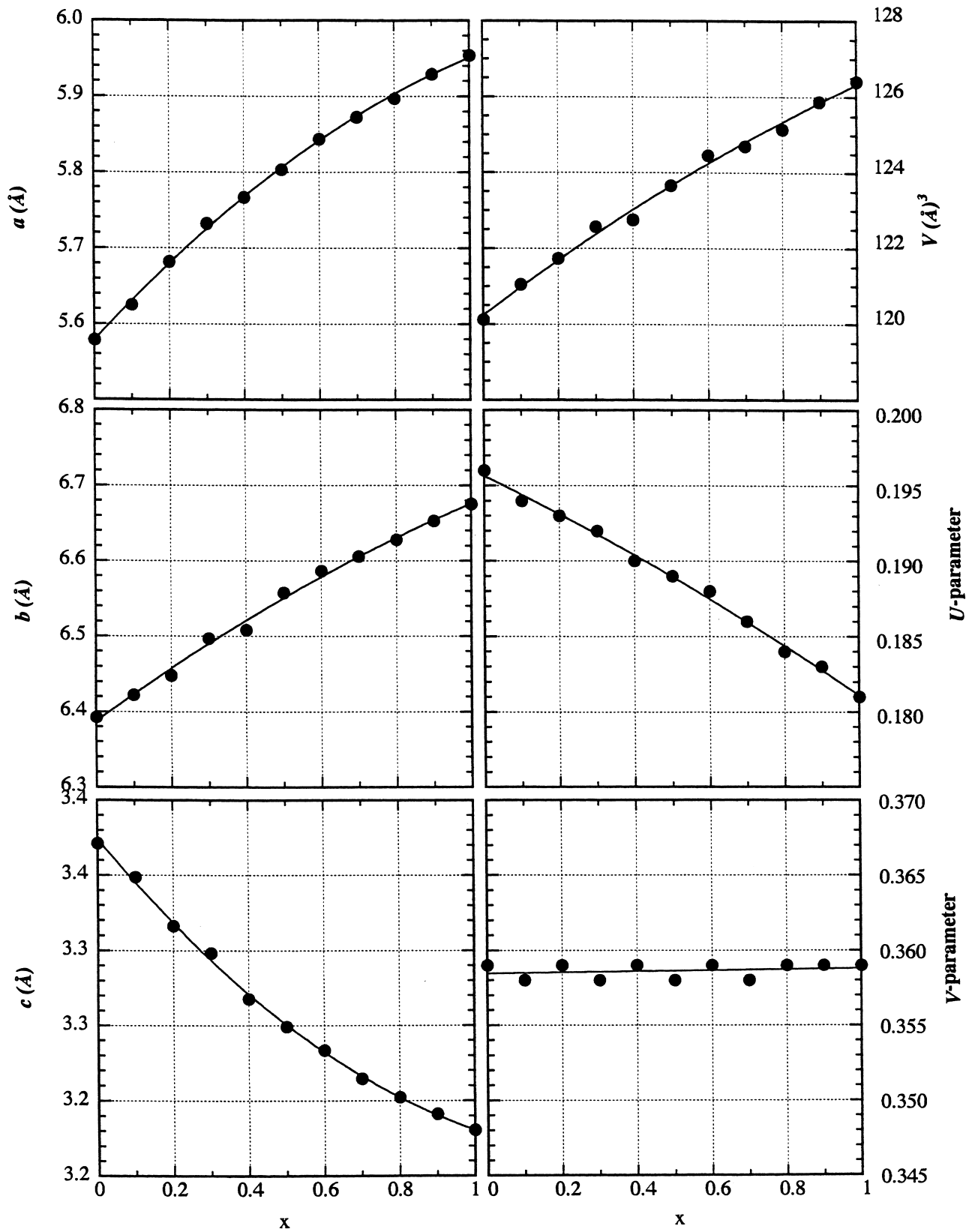


Fig. 2. Composition ( $x$ ) dependence of lattice parameters  $a$ ,  $b$ ,  $c$ , position parameters  $u$  and  $v$  and volume of unit cell ( $V$ ) for  $\text{Co}_{1-x}\text{Ru}_x\text{Sb}_2$  ( $0 \leq x \leq 1$ ) at room temperature.

Table 1  
Lattice parameters of  $\text{Co}_{1-x}\text{Ru}_x\text{Sb}_2$  ( $0 \leq x \leq 1.0$ )

Composition $x$	Lattice parameter (Å)			$V$ (Å <sup>3</sup> )	$\beta$	$u^a$	$v^a$	M–R <sup>b</sup> (Å)
	$a$	$b$	$c$					
0	5.5788	6.3925	3.3711	120.12	89.65	0.196	0.359	2.542
0.1	5.6251	6.4223	3.3488	121.05	89.84	0.194	0.357	2.545
0.2	5.6820	6.4481	3.3162	121.74	90.00	0.193	0.359	2.561
0.3	5.7320	6.4967	3.2982	122.57	90.00	0.192	0.358	2.573
0.4	5.7665	6.5079	3.2677	122.75	90.00	0.190	0.359	2.580
0.5	5.8035	6.5578	3.2493	123.66	90.00	0.189	0.358	2.591
0.6	5.8439	6.5863	3.2335	124.46	90.00	0.188	0.359	2.607
0.7	5.8727	6.6058	3.2146	124.70	90.00	0.186	0.358	2.605
0.8	5.8968	6.6278	3.2023	125.15	90.00	0.184	0.359	2.615
0.9	5.9289	6.6530	3.1912	125.88	90.00	0.183	0.359	2.623
1.0	5.9540	6.6756	3.1805	126.41	90.00	0.181	0.359	2.628

<sup>a</sup>  $u$  and  $v$ , position parameters in the orthorhombic unit cell.

<sup>b</sup> M–R, nearest distance between metal and metalloid.

were mixed in desired compositions and were sealed in evacuated silica tubes. Then, they were heated up to 700–800°C for about 7 days. After, the ingots were pulverized, mixed, sealed again in evacuated silica tubes and heated at 700°C for 5 days and slowly cooled. The heat treatment was repeated for each sample until it exhibited a single phase.

Powder X-ray diffraction measurements were carried out using Cu  $K\alpha$  radiation. All diffraction lines for the prepared samples were indexed according to the orthorhombic marcasite structure and related monoclinic distortion. An extra line showing the existence of impurity phase in X-ray patterns was not observed.

The samples for electrical measurements were prepared by heating at 650°C after pressing powders into a disk and then by cutting into a bar of 1×2×7 mm. Electrical resistivity was measured by an ordinary four-probe technique using mechanical positional point contacts. Hall coefficient was measured under magnetic fields of 5 kOe and 10 kOe. Thermoelectric measurements were carried out with Copper-Constantan thermocouples in direct contact with the samples. The temperature difference across a sample was 3–7°C. Details of experimental procedure are given in Ref. [13].

### 3. Results and discussion

Fig. 2 shows the lattice parameters  $a$ ,  $b$ ,  $c$ , position parameters  $u$  and  $v$  and volume of unit cell  $V$  as a function of the Ru content  $x$ , respectively. The values of  $a$ ,  $b$ ,  $c$ ,  $V$ ,  $u$ ,  $v$  and  $\beta$  are given in Table 1. In the figures and the table, the lattice parameters are expressed with the orthorhombic setting. The lattice parameters of  $\text{CoSb}_2$  and  $\text{RuSb}_2$  in the table are identical to that for  $\text{CoSb}_2$  reported

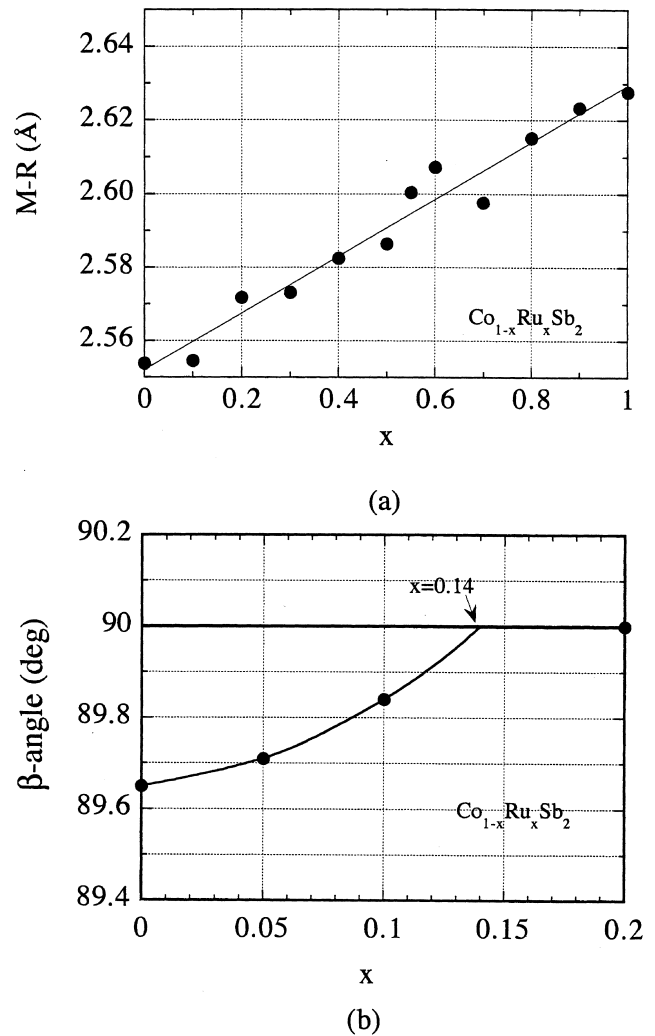


Fig. 3. Composition ( $x$ ) dependence of nearest atomic distance of metal (M)–metalloid (R) and the  $\beta$  angle of the marcasite-type structure for  $\text{Co}_{1-x}\text{Ru}_x\text{Sb}_2$  ( $0 \leq x \leq 1$ ) at room temperature; (a) M–R and (b)  $\beta$ .

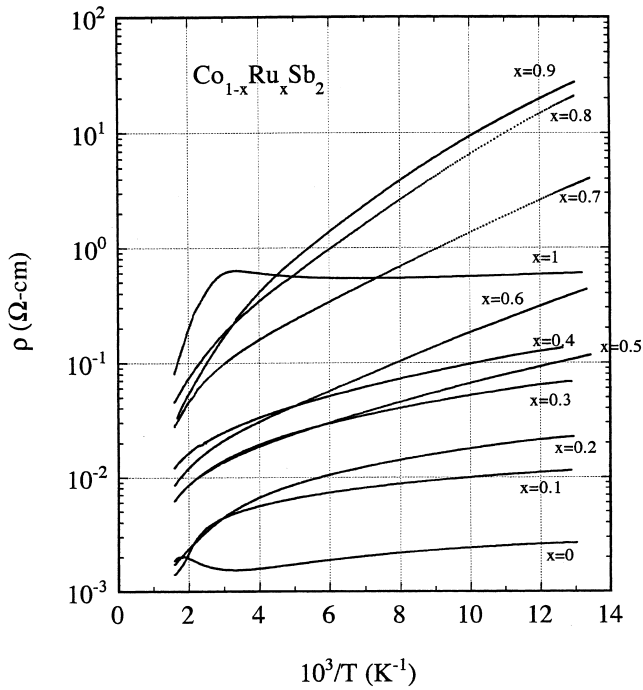


Fig. 4. Temperature dependence of resistivity ( $\rho$ ) of  $\text{Co}_{1-x}\text{Ru}_x\text{Sb}_2$  ( $0 \leq x \leq 1$ ).

by Terzief [8] ( $a=5.5789 \text{ \AA}$ ,  $b=6.387 \text{ \AA}$ ,  $c=3.376 \text{ \AA}$ ) and for  $\text{RuSb}_2$  reported by Holseth [14] ( $a=5.9524 \text{ \AA}$ ,  $b=6.6737 \text{ \AA}$ ,  $c=3.1803 \text{ \AA}$ ). As shown in Fig. 2,  $a$  and  $b$  decrease with increasing  $x$ . However,  $c$  (the nearest atomic metal distance (M–M)) decreases more sharply than those of  $a$  and  $b$ , with increasing  $x$ .  $V$  decreases linearly with  $x$ . The parameter  $u$  decreases slightly with  $x$ , but the  $v$ -parameter does not change with  $x$ . Fig. 3a and b show the composition dependence of nearest atomic distance between metal and metalloid (M–R) and the  $\beta$  angle, respectively, which is equal to  $90^\circ$  for the orthorhombic unit cell and smaller than  $90^\circ$  for the monoclinically

Table 2  
Electrical properties of  $\text{Co}_{1-x}\text{Ru}_x\text{Sb}_2$  ( $0 \leq x \leq 1$ )

Composition $x$	$\rho$ (300 K) ( $\Omega \text{ cm}$ )	$S$ (300 K) ( $\mu\text{V/K}$ )	$R_H$ (80 K) ( $\text{cm}^3/\text{C}$ )	$\mu$ (80 K) <sup>a</sup> ( $\text{cm}^2/\text{V s}$ )	$E_g^b$ (eV)
0	0.0015	+26	$+1.8 \times 10^{-1}$	h 70	0.15
0.1	0.0049	+3	$+6.0 \times 10^{-3}$	h 0.54	0.17
0.2	0.0052	-13	$-1.5 \times 10^{-3}$	e $8.9 \times 10^{-3}$	0.14
0.3	0.016	-13	$-2.5 \times 10^{-3}$	e $2.6 \times 10^{-3}$	0.14
0.4	0.028	-14	$+3.8 \times 10^{-3}$	h $2.9 \times 10^{-4}$	0.13
0.5	0.015	-19	$+6.2 \times 10^{-3}$	h $6.4 \times 10^{-2}$	–
0.6	0.024	-35	$-7.5 \times 10^{-3}$	e $2.2 \times 10^{-2}$	0.18
0.7	0.12	-72	$-7.6 \times 10^{-2}$	e $2.2 \times 10^{-2}$	0.22
0.8	0.23	-138	-0.61	e $3.0 \times 10^{-2}$	0.19
0.9	0.22	-233	-5.8	e 0.25	0.29
1.0	0.63	-274	-1.3	e 6.1	0.39

<sup>a</sup>  $\mu$ , mobility; e, electron; h, hole.

<sup>b</sup>  $E_g$ , intrinsic energy gap.

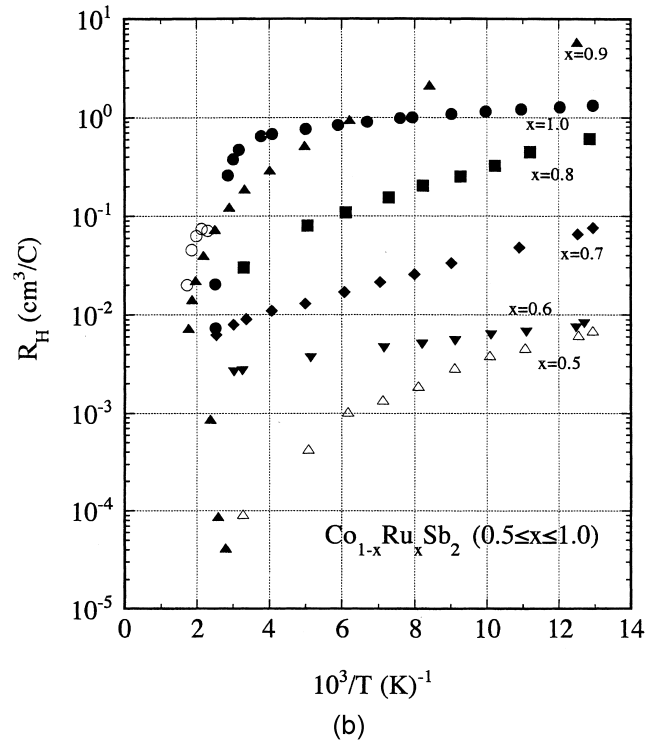
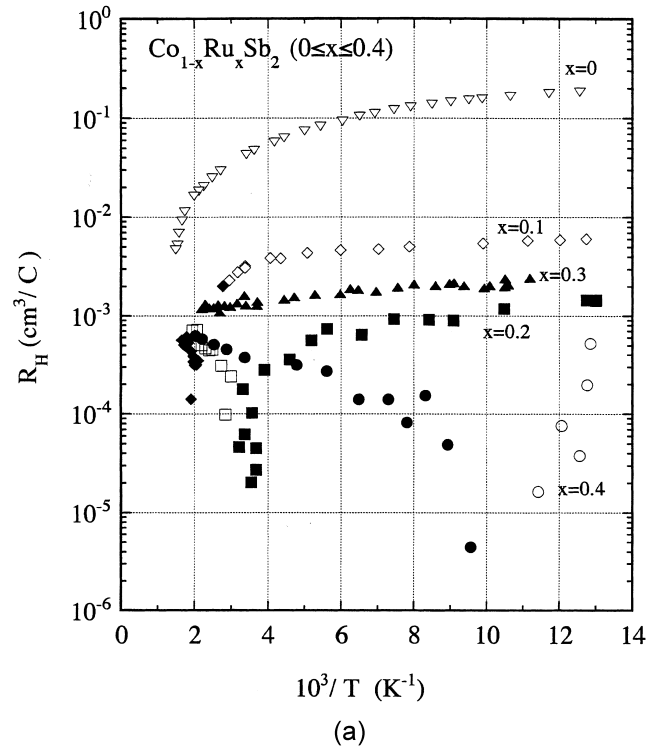


Fig. 5. Temperature dependence of Hall coefficient ( $R_H$ ) of  $\text{Co}_{1-x}\text{Ru}_x\text{Sb}_2$  ( $0 \leq x \leq 1$ ); (a) for ( $0 \leq x \leq 0.4$ ) and (b) for ( $0.5 \leq x \leq 1.0$ ). Open symbols are positive and closed symbols are negative.

distorted cell. As shown in Fig. 3b, the monoclinic distortion from the orthorhombic marcasite structure decreases gradually and disappears at about  $x=0.14$ . The M–M distance ( $\equiv c$ ) decreases about 6% and M–R distance increases about 3% from  $x=0$  to  $x=1$ .

Fig. 4 shows the resistivities of the examined  $\text{Co}_{1-x}\text{Ru}_x\text{Sb}_2$  ( $0 \leq x \leq 1$ ) samples as a function of temperature. All  $\log \rho - 1/T$  curves show semiconductive temperature variation. In the high temperature region,  $\log \rho$  decreases steeply and linearly with  $1/T$ . Using  $\log \rho \sim \Delta E / 2kT$  for intrinsic conduction, we derive a gap  $\Delta E = 0.15$  eV for  $\text{CoSb}_2$  and  $\Delta E = 0.40$  eV for  $\text{RuSb}_2$ . The composition dependence of the energy gaps calculated for  $\text{Co}_{1-x}\text{Ru}_x\text{Sb}_2$  is shown in Table 2 with some other electrical properties. The band gaps are almost constant for  $x < 0.5$  and increase sharply for  $x > 0.5$ .

Fig. 5a and b show  $R_H$  vs.  $1/T$  curves. As it can be seen,  $R_H$  at 77 K is positive (p) for  $x=0, 0.4, 0.5$  and negative (n) for other compositions; the absolute value of  $R_H$  decreases for  $0 \leq x \leq 0.4$  and increases for  $0.5 \leq x \leq 1.0$ .  $R_H$  changes its sign with increasing temperature in the examined range of measurements as follows; n for  $x=0$ ; n  $\rightarrow$  p for  $x=0.1, 0.2$ ; n for  $x=0.3$ ; p  $\rightarrow$  n for  $x=0.4, 0.5$ ; n for  $x=0.6, 0.7, 0.8, 0.9$ ; p  $\rightarrow$  n for  $x=1.0$ . It can be noted that n-type conduction for  $0.6 \leq x \leq 0.9$  is due to excess electrons by substituting Co for Ru in  $\text{RuSb}_2$ . Moreover, it can be seen that the value of  $\log |R_H|$  for  $x=0.1, 0.2, 0.4$  increases linearly with  $1/T$  in the high temperature range. The value of the mobility ( $\mu$ ) at 80 K was calculated by using the relation  $\mu = |R_H|/\rho$ . We obtained  $\mu = 70 \text{ cm}^2/\text{V s}$

for the positive hole in  $\text{CoSb}_2$  and  $\mu = 6.1 \text{ cm}^2/\text{V s}$  for the electron in  $\text{RuSb}_2$ . The composition dependence of the  $\mu$  obtained at 80 K is shown in Table 2. The value of  $\mu$  for  $0.2 \leq x \leq 0.8$  is very small ( $\sim 10^{-2} \text{ cm}^2/\text{V s}$ ) compared with those for  $x=0$  ( $\text{CoSb}_2$ ) and  $x=1$  ( $\text{RuSb}_2$ ).

Fig. 6 shows the thermoelectric power ( $S$ ) of the  $\text{Co}_{1-x}\text{Ru}_x\text{Sb}_2$  ( $0 \leq x \leq 1$ ) samples as a function of temperature. The  $S$  value for  $\text{CoSb}_2$  varies from positive to negative with increasing temperature. As seen in the figure,  $S$  for  $0 \leq x \leq 0.6$  has a small negative value in the whole temperature region. The value of  $S$  for  $0.7 \leq x \leq 1.0$  varies largely with increasing temperature.

It should be noticed that all prepared samples are semiconductive in spite of changing the valence electrons, gradually, by substituting Ru for Co, as mentioned above. These experimental results cannot be understood on the

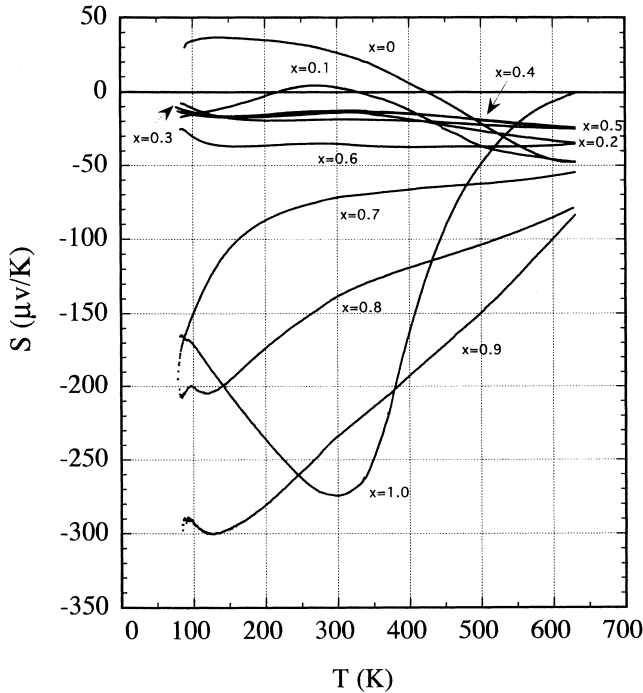


Fig. 6. Temperature dependence of thermoelectric power ( $S$ ) of  $\text{Co}_{1-x}\text{Ru}_x\text{Sb}_2$  ( $0 \leq x \leq 1$ ).

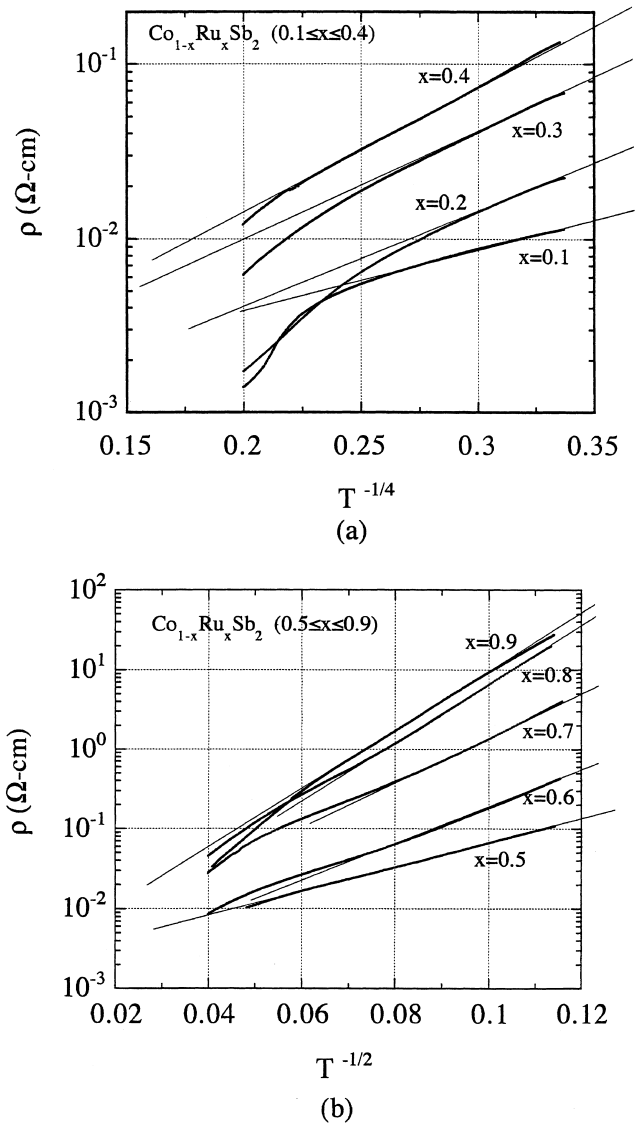


Fig. 7.  $\log \rho$  vs.  $T^{-1/4}$  and  $\log \rho$  vs.  $T^{-1/2}$  curves of  $\text{Co}_{1-x}\text{Ru}_x\text{Sb}_2$  ( $0.1 \leq x \leq 0.9$ ); (a) for ( $0.1 \leq x \leq 0.4$ ) and (b) for ( $0.5 \leq x \leq 0.9$ ).

basis of the band model, used for the explanation of semiconductivity of  $\text{CoSb}_2$  and  $\text{RuSb}_2$ .

We have examined the  $T^{-1/4}$  and  $T^{-1/2}$  temperature dependences of  $\log \rho$ . The results are shown in Fig. 7a and b. As shown in the figure,  $\log \rho$  is proportional to  $T^{-1/4}$  for  $0.1 \leq x \leq 0.4$  and to  $T^{-1/2}$  for  $0.5 \leq x \leq 0.9$  in the lower temperature region. These results correspond to a temperature dependence of  $\rho$  which can be expressed as  $\rho = \rho_0 \exp(T_0/T)^{1/4}$  for  $x \leq 0.4$  and  $\rho = \rho_0 \exp(T'_0/T)^{1/2}$  for  $x \geq 0.5$ . The temperature variations of  $\rho$  are the same as those of the variable range hopping (VRH) conduction in the impurity conduction range of semiconductors [16,17]. The relation of  $\log \rho \propto T^{-1/4}$  was given by Mott [15] and that of  $\log \rho \propto T^{-1/2}$  by Efros and Shklovsky [18]. The characteristic temperature  $T_0$  and  $T'_0$  increase with decrease of the localization length of impurity states. The values of  $T_0$  and  $T'_0$  obtained for the present system are greater by an order of hundreds than those of VRH in ordinary semiconductors. It is considered that the large values of  $T_0$  and  $T'_0$  are ascribed to strong localization of d-states in  $\text{Co}_{1-x}\text{Ru}_x\text{Sb}_2$ .

## References

- [1] R.N. Kuz'min, N.N. Zhuravlev, S.A. Losievskaya, *Sov. Phys. Cryst.* 5 (1960) 202.
- [2] K. Kjekshus, T. Rakke, A.F. Andersen, *Acta Chem. Scand.* A31 (1977) 253.
- [3] K. Kjekshus, T. Rakke, *Acta Chem. Scand.* A31 (1977) 517.
- [4] L.D. Dudkin, N.Kh. Abrikosov, *Russ. J. Inorg. Chem.* 2 (1957) 325.
- [5] T. Siegrist, F. Hulliger, *J. Solid State Chem.* 63 (1986) 23.
- [6] T. Caillat, A. Bolshchevsky, J.P. Fleurial, *AIP Conf. Proc. (USA)* 271 (1993) 771.
- [7] T. Caillat, *J. Phys. Chem. Solids* 59 (1998) 61.
- [8] P. Terzieff, H. Schicketanz, *J. Alloys Comp.* 232 (1996) 26.
- [9] F. Hulliger, E. Mooser, *J. Phys. Chem. Solids* 26 (1965) 429.
- [10] G. Brostigen, A. Kjekshus, *Acta Chem. Scand.* 24 (1970) 2993.
- [11] J.B. Goodenough, *J. Solid State Chem.* 5 (1972) 144.
- [12] A.K.L. Fan, G.H. Rosenthal, H.L. Mckinzie, A. Wold, *J. Solid State Chem.* 5 (1972) 136.
- [13] T. Harada, *J. Phys. Soc. Jpn.* 67 (1998) 1352.
- [14] H. Holseth, A. Kjekshus, *Acta Chem. Scand.* 22 (1968) 3284.
- [15] N.F. Mott, *Metal-Insulator Transitions*, Taylor and Francis, 1974.
- [16] M. Pollak, B. Shklovskii, *Hopping Transport in Solids*, North-Holland, 1991.
- [17] N.F. Mott, *J. Non-Cryst. Solids* 1 (1968) 1.
- [18] A.L. Efros, B.I. Shklovskii, *J. Phys. C* 8 (1975) L49.